# Sustainable RF Wireless Power Transfer and Energy Harvesting and Their Applications

Mahmoud Wagih and Dieff Vital

In the last two decades, energy harvesting technologies have generated significant interest, attributed to the decline in the power consumption of digital electronics. Electromagnetic (EM) power harvesting and delivery mechanisms, across the frequency spectrum, have been researched. In this chapter, we start by introducing the state-of-the-art in RF-enabled energy harvesting and wireless power transfer (WPT) technologies. Moving from device-level to system-level perspectives, the key enabling platforms are discussed with their environmental impact evaluated to assess their potential use enablers of net-zero intelligent systems.

## 1 RF Power Harvesting and Conversion Methods

The invention of the rectifying antenna (rectenna) in the 1950s enabled microwave WPT to high-power unmanned autonomous vehicles (UAVs) based on highly directional antenna arrays [8]. Shortly afterwards, the idea of beaming solar power from satellites, using microwaves, emerged [39]. In modern times, RF WPT has found applications and continues to attract research interest, ranging from harvesting the ambient emissions [38], to powering soft biomedical circuits [19]. To enable RF energy harvesting and WPT to contribute to a 6G-enabled net-zero, these systems need to maintain a high end-to-end efficiency. The efficiency in a WPT system is given by:

$$\eta = \underbrace{\frac{P_{RF}}{P_{DC}}}_{e_1} \times \underbrace{\frac{P_{RF-RX}}{P_{RF-TX}}}_{e_2} \times \underbrace{\frac{P_{DC}}{P_{RF}}}_{e_3} \times \underbrace{\frac{P_{DC-Load}}{P_{DC-RX}}}_{e_4}. \tag{1}$$

where $e_1$ corresponds to the transmitter 's DC to RF conversion efficiency (mostly limited by the power amplifiers), $e_2$ is the efficiency of the wireless link, including antennas, $e_3$ is the rectifier's RF to DC power conversion efficiency, and finally $e_4$ is the DC-DC conversion and utilization efficiency, which includes losses in any power management or energy storage devices.

### 1.1 Device-Level Considerations: Rectifiers

When harvesting wireless power, the losses in the diodes often dominate the power dissipation in the receiver [10]. Therefore, to achieve a high end-to-end efficiency, efficient rectifier devices are required. Rectifiers are, however, highly non-linear components, and their power conversion efficiency (PCE) is bounded by two device parameters. First, the forward voltage drop across the diode's junction limits the PCE at low RF input levels. To explain, the antenna can be visualized as a voltage source with a given characteristic impedance. Therefore, a low forward voltage drop enables low input voltages to be rectified efficiently [44]. On the other hand, at high power levels, the breakdown voltage of the diodes limits the maximum DC voltage output. When the RF input power exceeds the breakdown voltage of the diode, the DC output (for a single-series rectifier) saturates around the breakdown voltage of the diode. This is attributed to the reverse leakage.

### 1.1.1 Rectifier Selection and Large-Signal Design

The effect of such efficiency bounds can be visualized in Figure 1 [22]. A higher incident power density, at the rectenna's aperture, increases the received power level and consequently the input to the rectifier. Therefore, each of the rectennas compared in Figure 1 achieves a high PCE in a very narrow input range, which highlights the significance of selecting a suitable rectification device based on the application.

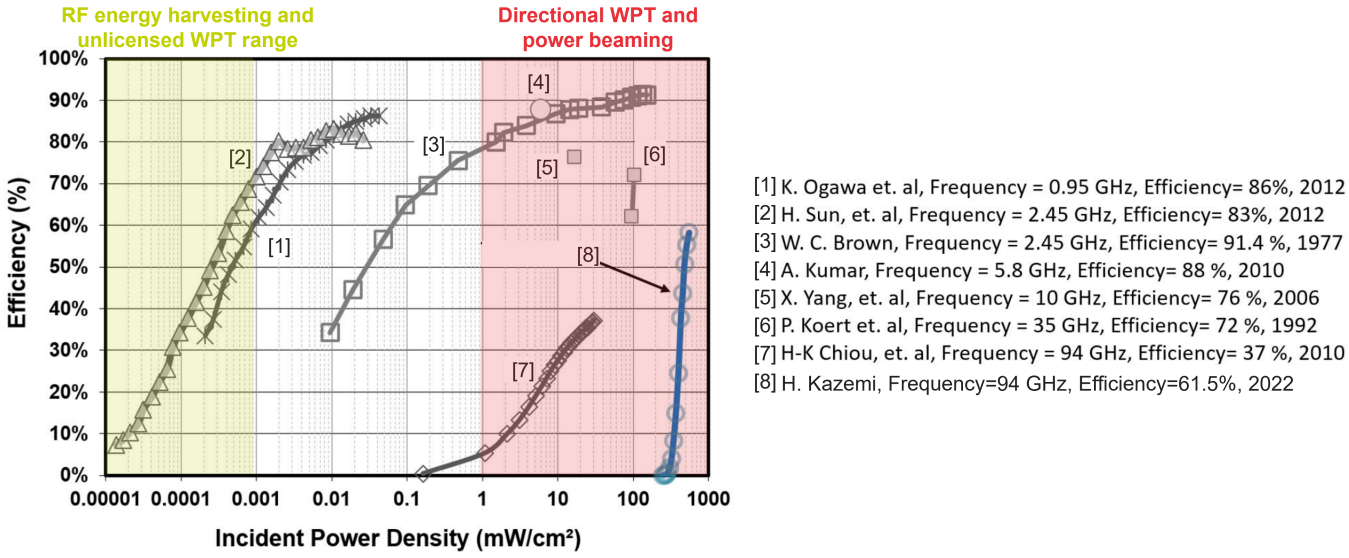


Figure 1: Comparison of the RF to DC of various rectifiers and rectennas from 2.4 to 94 GHz, showing the efficiency bounds at different ends of the RF power spectrum; adapted from [22] (CC-BY).

In low-power RF energy harvesting applications, such as recycling the freely available power from cellular networks [15,38], a diode with an extremely low forward voltage is often chosen. In addition, the non-linear large-signal impedance matching is optimized for a low RF input to maximize the PCE and minimize reflections at the desired power level, often between −30 and −20 dBm [2]. These requirements also apply to WPT in the license-free spectrum, where the equivalent isotropic radiated power (EIRP) limits are typically under 4 W for frequencies below 2.4 GHz, depending on the geographical region. To illustrate, at a 10 m distance, in line-of-sight, from a 3 W 915 MHz transmitter, the incident power density is approximately around 0.2 µW/cm$^2$; as previously seen in Figure 1, a PCE under 50% is typically expected at frequencies around 2.4 GHz or lower, which indicates the significance of effective rectifier and antenna design.

On the other hand, high-power WPT applications expect a high-power density microwave beam to be directed at the rectenna element or array. Therefore, high-breakdown voltage diodes are selected. In high-power WPT research, higher frequencies in the mmWave spectrum are used, as seen in Figure 1, to enable more directional antennas in the same physical area [59]. The earliest mmWave rectenna development by Koert and Cha were aimed at power beaming applications in space, where atmospheric attenuation of mmWave signals does not represent a problem [24]. Kazemi demonstrated a rectenna operating 94 GHz with the highest efficiency and power-handling, as seen in Figure 1 based on Gallium Nitride (GaN) diodes.

The design of an RF rectifier is often carried out with the aid of a non-linear circuit simulator. Steady-state harmonic balance simulations are typically used to model rectifiers, where the non-linear impedance response of the diodes can be simulated. Figure 2(a) shows a coplanar layout of a sub-1 GHz rectifier based on commercial Schottky diodes. The antenna is modelled as the power source with a complex characteristic impedance. Similar to source- and load-pull tuning in an RF power amplifier, the input impedance of the rectenna, i.e. the antenna's impedance, is tuned to maximize the PCE at the target frequency. The load impedance is also tuned which can affect both the diode's impedance and its maximum-achievable PCE [57].

Imperative to efficient rectifier design and matching is the accurate modelling the rectifier's layout. While the traces shown in Figure 2(a) are significantly smaller than the wavelength, they can significantly change the optimum input

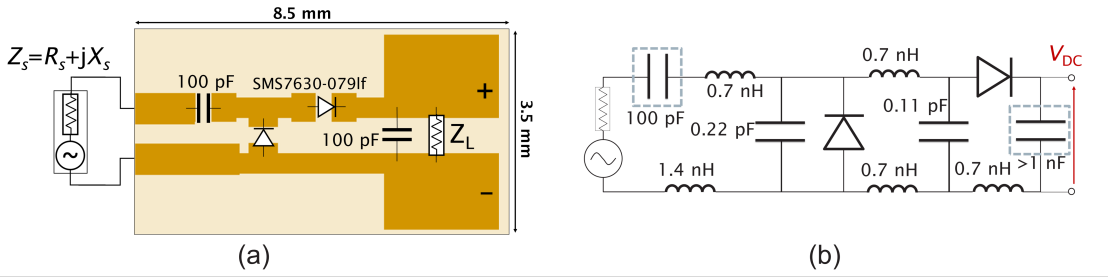


Figure 2: A non-linear harmonic balance simulation model of a sub-1 GHz rectifier: (a) The layout of a coplanar standard voltage doubler rectifier, with the antenna modeled as a voltage source with a complex impedance [57]; (b) the equivalent circuit model of the rectifier's traces [52].

impedance of the rectifier. Figure 2(b) shows the closed-form equivalent circuit model of the layout, used in optimizing the rectifier [52]. In addition to equivalent circuit models, electromagnetic co-simulation can be used to model the layout effects and incorporate them into the harmonic balance simulation flow.

The dependence of the rectifier's efficiency on the input impedance is illustrated in Figure 3, based on harmonic balance simulations (using Keysight Advanced Design Systems). The imaginary component of the input impedance $X_S$ directly matches the capacitive component of the rectifier's impedance $X_R$. Therefore, a highly resonant response is observed in the PCE-$X_S$ relation. On the other hand, once the source matched the rectifier's reactance, $X_S$=$X_R^*$, the real impedance-PCE relation resembles the maximum power transfer relation. At this frequency, where $X_S$=$X_R^*$, both the antenna and the rectifier can be considered as a resistive source and load, respectively, and therefore, the DC power output follows the maximum power transfer relation. To ensure the rectifier is matched to achieve the highest possible PCE, the $X_S$, $R_S$, and $Z_L$ tuning process should be carried out iteratively to account for the impedance mismatches and ensure the observed response corresponds to the anticipated RF power level at the diodes' junctions.

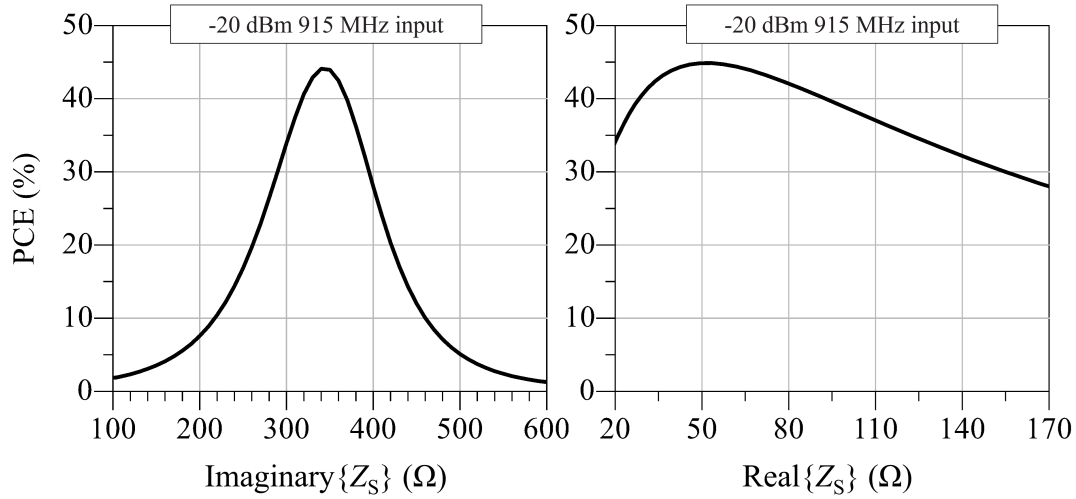


Figure 3: The rectifier's PCE as a function of the antenna's input impedance, illustrating the co-design process of an antenna and a rectifier for high-efficiency sub-1 GHz WPT at low power levels [57].

### 1.1.2 On-chip and fully-integrated solutions

In addition to Schottky-based rectennas, a plethora of RF energy harvesters and RF to DC charge-pumps have been implemented in ICs based on standard Complementary Metal Oxide Semiconductors (CMOS) processes. With UHF RFID being the largest commercial driver of RF rectifier circuits, multi-stage voltage multiplier circuits have been widely demonstrated in a variety of CMOS processes [44]. The main advantage of CMOS-integrated rectifiers is the ability to

implement them in a relatively small chip area (under 100×100 µm$^2$), alongside the digital transponder circuitry and backscattering modulator of the RFID IC.

From a rectification perspective, the same PCE bounds exist, i.e. the rectifier will be limited by the forward voltage drop across the diode-connected transistors, as well as the breakdown voltage of the devices. However, rectifiers can be implemented based on different topologies that extend beyond diode-connected transistors. An example is the cross-coupled rectifier [25], shown in Figure 4(a). In a cross-coupled rectifier, four transistors are differentially driven using the RF input from the antenna. The differential input biases the devices and allows reduced forward voltage losses, enabling the cross-coupled rectifier to achieve a higher sensitivity than its diode-connected transistor counterpart.

Several rectifiers have later been reported based on modified differentially-driven topologies, where the threshold voltage of the devices is dynamically changed to improve the rectifier's sensitivity, efficiency, and dynamic range. The rectifier shown in Figure 4(b) was proposed achieving over 80% at 433 MHz down to −19 m [4]. The −19 dBm would typically correspond to an available power density under 0.2 µW/cm$^2$ assuming an omnidirectional rectenna is used. Recalling Figure 1, the state-of-the-art PCE for such a lower power level, using discrete Schottky diodes, is under 50%, which shows the advantage of adopting low-threshold rectifier topologies, in modern CMOS processes, along with optimal device-sizing and threshold adjustment techniques.

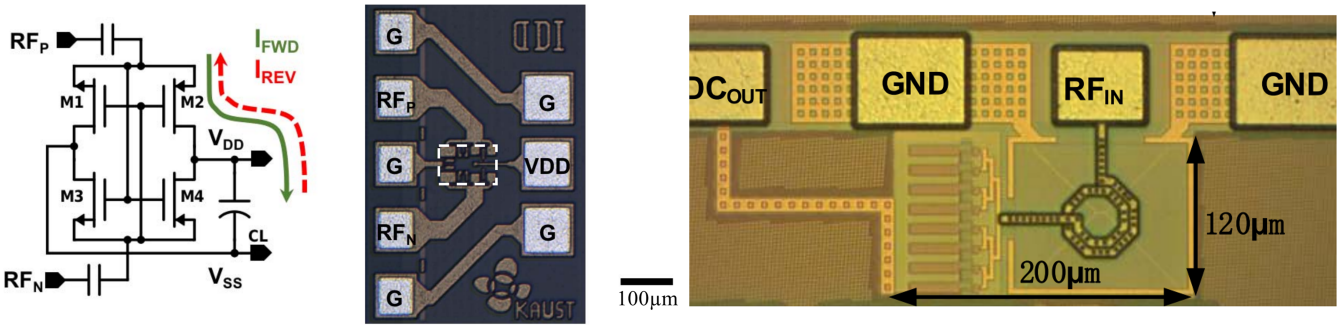


(a) (b) (c)

Figure 4: Fully-integrated rectifier circuits in CMOS processes: (a) a single stage of the cross-coupled threshold-cancellation rectifier; (b) chip micrograph of a high-sensitivity and efficiency 433 MHz on-chip rectifier; (a) and (b) taken from [4] (CC-BY); (c) a 57-64 GHz multi-stage mmWave rectifier; taken from [11] (CC-BY).

In addition to improving the sensitivity and the large-scale integration, moving to fully-integrated rectifiers is particularly attractive at mmWave frequencies [56]. To explain, the majority of mmWave rectennas based on discrete diodes use compound semiconductor, namely Gallium Arsenide (GaAs), diodes [59]. Such devices require additional electrostatic discharge (ESD) protection as well as careful handling and special assembly flows [26]. Extending mmWave rectennas beyond research demonstrators to pervasive energy harvesting devices requires lower cost rectifier devices which can be robustly integrated with other components. As a result, mmWave CMOS rectifiers are a prime candidate for enabling future mmWave energy harvesting systems, which can co-exist in 6G networks creating both information and power grids [23].

In [11], a multi-stage rectifier was proposed for a metres-range mmWave WPT system, operating in the 60 GHz license-free band. Owing to the high frequency of operation, the rectifier's inductive matching network was integrated on the same chip, where the matching inductor is visible in Figure 4(c). A power divider is then used to evenly feed the voltage multiplier's stage, enabling the rectifier to achieve a high sensitivity down to −6 dBm. Such multi-stage design will be challenging to implement at mmWave frequencies using discrete parts due to the added parasitics of the packaging, assembly, and layout, which highlights the benefits of CMOS integration for mmWave rectifiers and energy harvesters.

### 1.1.3 Emerging Solution-Processed Electronics

A key bottleneck in creating sustainable wireless electronic systems is the heavy reliance on micro- and nano-scale semiconductor devices in Silicon or group III-V processes. The energy and water consumption of the semiconductor foundries

as well as the heavy reliance on critical and rare elements can be minimized in certain applications by adopting alternative devices which can be used at GHz frequencies [14].

Processing semiconductors, on a wafer scale, from a solution could reduce the energy and scarce elements required to fabricate the diodes required in RF rectennas. All-flexible rectennas have been demonstrated on flexible films at 2.4 GHz, demonstrating the feasibility of adopting large-area solution-processed devices in sustainable RF energy harvesting applications [63].

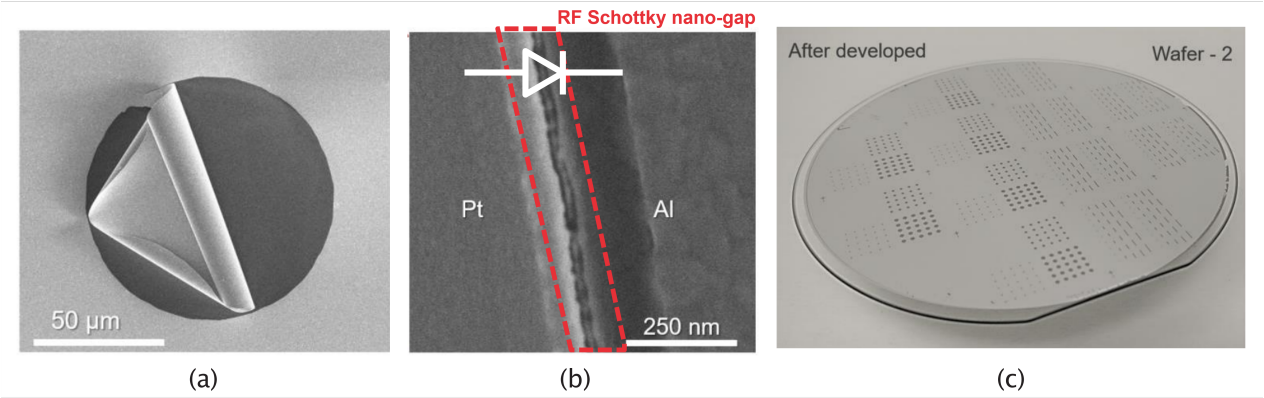


Figure 5: Sustainable and scaled-up fabrication of GHz-frequency diodes from a solution for RF energy harvesting: (a) self-forming process of the diodes to realize the nanogap; (b) SEM micrograph of the diode's nano-gap and its junction; (c) wafer-scale integration of rectifier diodes; adapted from [29] (CC-BY).

Recently, Zinc Oxide (ZnO)-based Schottky diodes were demonstrated on a wafer-scale, as shown in Figure 5, using adhesion lithography. These devices can be fabricated with an intrinsic cut-off frequency up to 100 GHz, showing their suitability for mmWave rectification. Such solution-processed components can be fabricated at a low temparature and are compatible with flexible susbtrates such as polyimide, enabling large-area monolithic integration of rectennas on flexible materials.

## 1.2 Antenna Topologies and Simultaneous Wireless Information and Power Transfer

Antennas play a fundamental role in efficient RF energy harvesting. While it can be assumed that any efficient radiator can act as an energy harvesting element when combined with an impedance-matched rectifier [60], energy harvesting-specific antenna design can enable more efficient harvesting and sustainable manufacturing of future 6G-based power supplies.

Microwave components, such as power amplifiers and detectors, are typically matched to a 50 Ω characteristic impedance to enable their integration into microwave systems. However, the RF energy harvester or the rectenna is a unique system where the output is in DC, and the standard approaches of RF combining may not apply. To explain, the most widely adopted form of a rectenna is the Ultra High Frequency (UHF) RFID tag. Each tag consists of a single discrete component, i.e. the RFID transponder IC, and a printed antenna, often implemented on a plastic film for ease of integration [32]. In an RFID tag, it is imperative to keep the cost down and, therefore, no additional matching components are used. Figure 6(a) the impedance matching interface between an antenna and a rectifier.

This approach of co-designing the antenna and the rectifier is key to sustainable and efficient RF energy harvesting. By combining the matching network's desired response within the antenna's input impedance, the insertion losses associated with matching using practical components [36] are mitigated. Furthermore, from a materials and manufacturing perspective, reducing the number of components required to realize the rectifier significantly lowers the environmental footprint of the energy harvester.

From an antenna perspective, minimizing the area required by the antenna or shifting to sustainable fabrication processes can further improve the sustainability of the RF energy harvester. In Figure 6(b) a rectenna integrated within the same area of a standard communication microstrip patch antenna is shown. This approach of utilizing shared-aperture antennas in energy harvesting enables the same circuit area, and subsequently, environmental impact, to be leveraged for both energy harvesting and wireless power harvesting [54, 55]. Furthermore, the antenna's environmental impact can

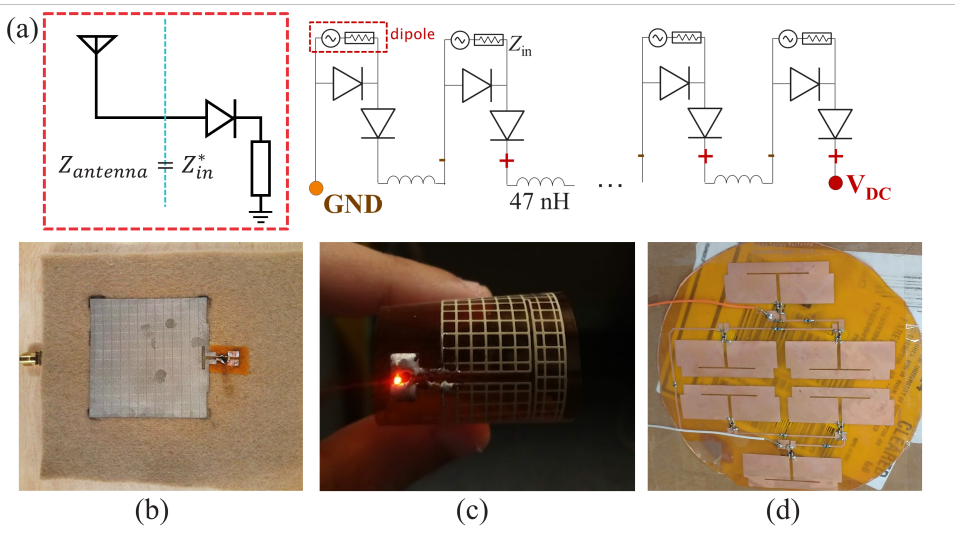


Figure 6: Directly matching rectifiers using complex-conjugate antennas: (a) an illustration of the impedance matching plane at the rectifier's input, and a simplified equivalent circuit scaled-up array implementation based on directly-matched rectenna elements [52]; (b) directly-matched wearable rectenna at 2.4 GHz [53]; (c) a sub-1 GHz dipole-based rectenna optimized for sustainable additive manufacturing [58]; (d) a six-element tightly-coupled rectenna array .

be reduced by utilizing additive fabrication processes. While additive manufacturing can impose additional geometrical constraints, particularly around the achieved resolution, it enables the rectennas to be realized on a plethora of large-area substrates. In Figure 6(c), a rectenna designed specifically for direct-write printing is shown; the antenna's radiator is meshed reducing the required conductive ink by up to 80% while maintaining the same RF energy harvesting efficiency.

Scaling co-designed rectennas to arrays can enable RF energy harvesting to operate at even lower power densities. As previously seen in Figure 1, it is very challenging to efficiently rectify incident power densities under 0.1 µW/cm$^2$ using an individual rectenna element such as [42]. Therefore, co-designed electrically-small rectenna elements can be arranged in DC-combining energy harvesting arrays, as seen in Figure 6 (a) and (d) [52]. By combining the DC output of tightly-coupled six rectenna elements which are originally designed to achieve a high DC sensitivity at low power levels, a complete Bluetooth Low Energy (BLE) sensing node can be powered from an ultra-low power density of 0.22 µW/cm$^2$. It is key to note that electrically-small antennas, such as wire-type dipoles, have a much larger effective area than their physical aperture [7], enabling them to act as area-efficient RF energy harvesting elements while maintaining physical compactness [28, 52]

Extending beyond WPT application to simultaneous wireless information and power transfer (SWIPT), new antenna topologies can enable energy harvesters to be integrated with information receivers. SWIPT networks represent a more sustainable approach to WPT and RF energy harvesting as the power can be directed to the desired user and the same carrier could potentially be used for both functions [37]. As seen in Figure 7, SWIPT can be implemented using multiple approaches including those based on the power conversion circuits and based on multiple antennas or multi-port individual antennas.

To enable a single antenna to simultaneously act as an information and power receiver a high isolation between the ports is required [55]. In addition, the antenna's power harvesting and information transmission radiation patterns should be mostly uncorrelated. On approach to achieve such high isolation between the ports is the use of hybrid couplers to connect the antenna to the rectifier [30]. By using a symmetrical coupler, the antenna can be operated either as a linearly or circularly-polarized receiver [30]. An alternative lower-complexity approach is using a shared-aperture antenna. The same radiating aperture can be excited using asymmetric feeding mechanisms. For example, one port could directly match the rectifier's impedance by utilizing an inductive feeding loop [53]. In addition, the radiator can be adapted to utilize different radiation modes for different applications [54].

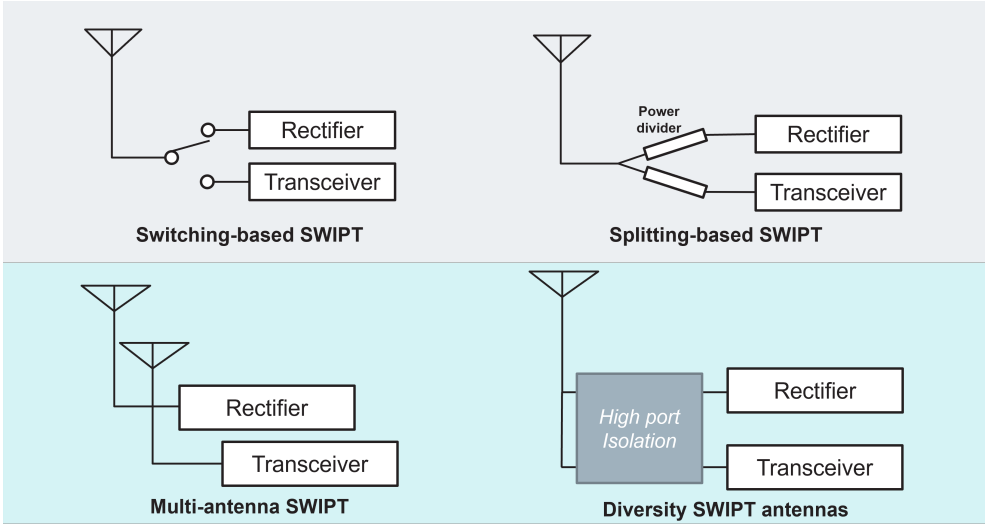


Figure 7: Antenna and circuit topologies for SWIPT including switching-based time-division, power-splitting, and antenna-based solutions.

# 2 Sustainable Wearable and Biomedical Applications and Approaches

Wearable technologies are a key application of RF energy harvesting and WPT. Human-centric connectivity is a key component of future 6G networks, and such systems need to be both energy-autonomous and user-friendly. This section overviews some of the wearable-specific design challenges and demonstrates how efficient and application-specific WPT systems can be developed for these wearables. Safety considerations for wearable WPT are finally addressed as an example of a highly-constrained WPT scenario in future 6G networks.

## 2.1 Materials and Fabrication Process

The high demand for wearable technology has a multifaceted field of applications starting from developing innovative and tactical gear for soldiers, smart clothing and clothing accessories for fitness assessment, and smart medical devices for smart, personalized, and connected health. Furthermore, in addition to the applications mentioned above, the users use electronic devices for day-to-day applications. Therefore, to properly develop these next-generation wearable electronic devices for day-to-day applications, it is crucial to consider the following parameters:

- *Flexiblity*: the devices should be conformal so that they can be easily bonded with any surfaces that undergo deformations like bending, twisting, and folding.
- *Comfort*: when the devices are embedded into clothing items, the bearer should not feel that something else is added to the clothes; hence, the integration should be seamless,
- *cost-efficiency*: one of the important requirements for the next generation of wearable devices is the affordability by every user regardless of their financial condition,
- *Ease of manufacturing*: to enable mass production, the devices should be simplistic so that fewer materials and a short turnaround time can be realizable,
- *Resilience to deformations*: as the bearer will be subject to all kinds of movements, the structures (devices) are expected to be resilient, which means their performance will not alter should they undergo such deformations. For that, crucial manufacturing parameters should be controlled to provide full flexibility to the devices while their RF performance is not compromised, and
- *Safety and bio-compatibility*: these devices will be antennas and RF circuits to transmit, receive, and convert RF signals. Therefore, mechanisms must be in place to eliminate the hazards that might result from human radiation exposure. For that, the choice of materials is essential.

Cutting-edge research will be carried out to deliver devices that can be seamlessly integrated into clothing or upholstery, with low loss for RF performance and excellent bio-compatibility. The latter will allow connected and personalized care where patients can access real-time information about their health and suggest prompt decisions only by wearing a piece of clothing that act like their regular day-to-day clothing items. Moreover, these clothing items will help space explorers and military personnel stay on duty. At the same time, their communications interfaces and tactical gears can automatically send and receive information, process it, and make decisions on their behalf. Since wearable devices are intelligent, they will trigger an alarm should something abnormal like an emergency happen. Wearables are closely related to sensing devices within the Internet of Things (IoT) and the Internet of Health Things (IoHT). These sensing devices are commonly used to measure metrics like heart rate and oxygen level, in defense for integrated communication interfaces and sensing tactical gears, in smart auto for sensor/antenna integrated car seats/belts, and in space for sensor-equipped space suits. Developing devices for medical applications bring about a specific set of challenges. These challenges are related to eliminating battery dependence and developing textile-based wireless power transfer, harvesting for monitoring, and sensing. The substrates used to develop these devices are breathable gauze fabrics. These fabrics are integrated well with conductive materials like copper and silver tapes integrated as well as the fabric substrates via stick-and-peel. carbon nanotubes, conductive ink that can be applied via screen printing or inkjet printing, conductive epoxies that can be manually applied onto the fabric substrates, and conductive threads that are interwoven via automated embroidery. Gauze fabrics are low-cost substrates already used to develop bandages and can be found almost at any fabric supplier. The conductive materials, however, have advantages and disadvantages that make them the best candidates to develop smart medical devices that those with low financial means can use. A breakdown of the characteristics of those materials is listed below:

1. **Textile: conductive threads (E-fibers)**

   (a) Shieldtex silver-plated polyamide thread (234/34-2 ply HCB)
   *Pros*: sheet resistivity 100Ω/m
   *Cons*: thick thread, limited resolution

   (b) Elektrisola-7 (silver-coated copper)
   *Pros*: improved resistivity 0.0171Ω/m, good RF conductivity (2.44 $\times 10^6$ S/m, fully flexible, suitable for RF applications, resilient to mechanical deformations (bending and twisting [46])
   *Cons*: No elastomer used

2. **Conductive printed ink: silver nanoparticles with or without polymeric binder**

   (a) JS-A211 (Novacentrix)
   *Pros*: easy to print on TPU, PET, polycarbonate
   *Cons*: direct printing on fabrics (e.g., denim, organza), too small to properly saturate/coat the textile fibers, vulnerable to mechanical deformations.

3. **Conductive Epoxy: silver with polymer binder**

   (a) nanoparticles
   *Pros*: ink-jet printing, fast sintering, R2R, volume resistivity :$< 3.1 \times 10^{-5} \Omega/m^3$
   *Cons*: cannot withstand repetitive mechanical deformations, not flexible (generate cracks under deformations) when used in hard-to-soft interconnections.

   (b) nanoflakes (CreativeMaterials 127-48)
   *Pros*: volume resistivity: $6.5 \times 10^{-5} \Omega/cm$, 82% of silver when cured, excellent crease resistance, excellent adhesion with fabrics, good to replace the solder in crack-free interconnects, fully flexible, good for hard-to-soft and soft-to-soft interconnections, suitable for RF applications in printed circuits, and washable textiles.
   *Cons*: conductivity improves with high curing temperature like 125°C.

(c) nanowires

*Pros*: superior conductivity under strain, shallow solid content to offer flexibility

*Cons*: nothing noticeable

(d) epoxy-graphene

*Pros*: low-cost, conformality, resilience to deformations (20000 cycles)

*Cons*: reasonably low conductivity compared to copper

4. **Copper and silver tapes [27]**

   *Pros*: high conductivity, homogeneous structure, biocompatible, integration with flexible substrates like fabrics, good recycling, long working life in normal operating conditions, excellent EMI and RFI shields to devices

   *Cons*: cracks formed after several cycles of bending, twisting, and folding, high production cost, high complexity of processes, high environmental impact, low corrosion resistance.

5. **Carbon nanotubes [27]**

   *Pros*: low density, excellent mechanical and thermal properties, excellent conductivity of up to 50000 $S.cm^{-1}$ (when doped with $HSO_3CL$ and $I_2$), 67 000 $S.cm^{-1}$, biocompatible, integrate with flexible substrates like fabrics, lightweight, low production cost, abundant availability of resources, low complexity of processing, good recycling, high corrosion resistance

   *Cons*: uncontrolled morphology (cause of limitation in electrical wiring applications).

The five categories of conductive materials listed above are used to realize conductive phases placed atop the substrates to build the RF structures for wearable applications. The category of conductive ink exhibits excellent conductivity and great integration with fabric substrates. However, when subject to mechanical deformations, cracks are formed, and the RF performance of the structures is therefore compromised. The conductive epoxies suffer either low conductivity or resilience to mechanical deformations. Carbon nanotubes have excellent electrical properties. However, to achieve conductivity as close as that of copper or aluminum, doping is required, and that would increase the manufacturing cost.

Copper/aluminum and silver tapes have the highest conductivity among the five categories of conductive materials.

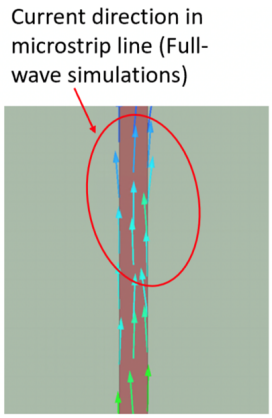


Figure 8: Illustration of the RF current flowing along the 90°-fill stitch Textile transmission line.

However, they cannot withstand repetitive mechanical deformation tests. In addition, any sharp object can poke the surfaces, and holes can be perforated throughout, which can compromise the conductivity of the conductive surfaces. The embroidered textile threads are the best candidates for conductive surfaces as they bode better with the substrate via the embroidery technique. The embroidery process allows interweaving to integrate the conductive yarn with the fabric substrate. The instrument used for the integration is any commercial embroidery machine that is easy to use, easy to embroider the structures, and does not require any professional training to operate the machine, which can help reduce manufacturing costs. For excellent RF performance of the embroidered structures, the design and manufacturing parameters should be controlled so that relevant tests about the robustness of the structures and their resilience to deformation can be performed and confirmed.

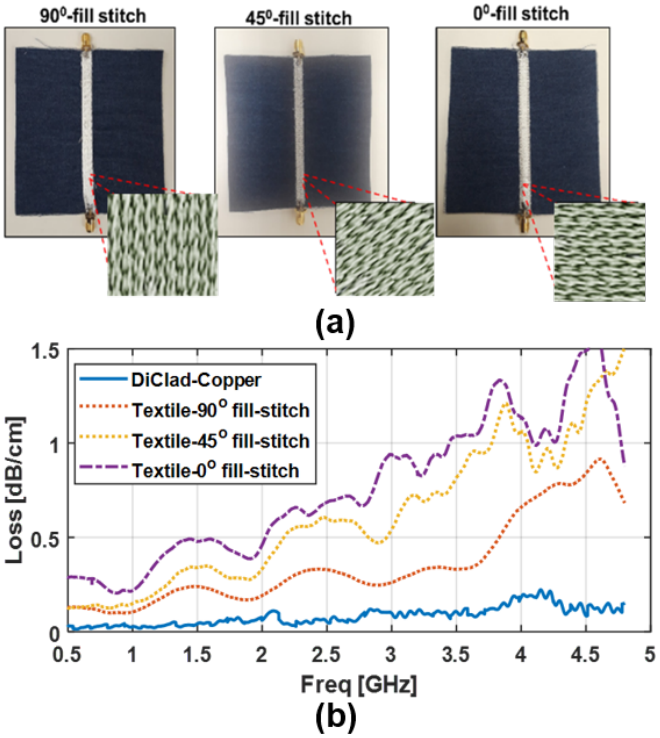


Figure 9: Loss-comparison of stitching patterns in textile-based transmission lines made of Elektrisola-7 embroidered onto denim fabric. (a) Photos of finished prototypes with three different embroidery patterns under study (angles are estimated between the thread and horizontal axis) and (b) Measured loss-performance of different patterns. (©2018 IEEE [50])

### 2.1.1 Optimization of embroidery parameters and RF Performance

Optimizing the embroidery parameters comes down to three key variables that include (1) the stitching pattern that corresponds to the embroidery direction of the conductive thread concerning the direction of the RF current (see Figure 8), (2) the thread density, which is the number of threads per unit length of stripline, and (3) the tension, which is a parameter straight out of the embroidery machine that is of the range of 0 to 9. The thread density parameter is important as it keeps the conductive surface almost intact when the structure is subject to mechanical deformations like bending, twisting, and folding. The tension parameter dictates how much the top thread (nonconductive thread in the embroidery machine) pulls the bottom threads (conductive threads from the bobbin). The latter can be controlled to ensure that the nonconductive and conductive threads can smooth the seam's surface without thread breakage. When strictly controlled, the thread tension and density will ensure deformation resilience. Here, the investigation started with the design and fabrication of four microstrip transmission lines (MTLs). The first is made of DiClad880 substrate ($\epsilon_r = 2.2$ and $\tan\delta = 0.009$), where copper is cladded on top of it. The other three are made of Elektrisola-7 embroidered onto denim fabric (Figure 9). When combined with a sticky stabilizer, the denim fabric has a dielectric constant $\epsilon_r = 1.67$ and a dielectric loss $\tan\delta = 0.07$. The stitching patterns used in the textile MTLs were the: (1) 90°-fill stitch, corresponding to aligning the embroidered conductive threads with the direction of the RF current, (2) 45°-fill stitch, which signifies that the conductive threads are embroidered at 45° concerning the direction of the RF current, and (3) 0°-fill stitch, which corresponds to embroidering the conductive threads perpendicularly to the direction of the RF current. The thread density was kept in the vicinity of 14 threads/mm to ensure excellent conductivity. The thread density was chosen to be 4 to allow for unrestricted movement of the embroidered threads under mechanical deformation influences. The DiClad880-MTL was prototyped using an LPKF milling machine, and two SMA connectors were attached at both ends of the transmission line for port excitation. The other three MTLs were prototyped by embroidering conductive threads known as *Elektrisola-7* onto the denim substrate. Two SMA connectors were soldered at both ends of each textile MTL for excitation (see Figure 9(a)). The scattering parameters of all four MTLs were measured using a Keysight PNA N5222B, and the loss

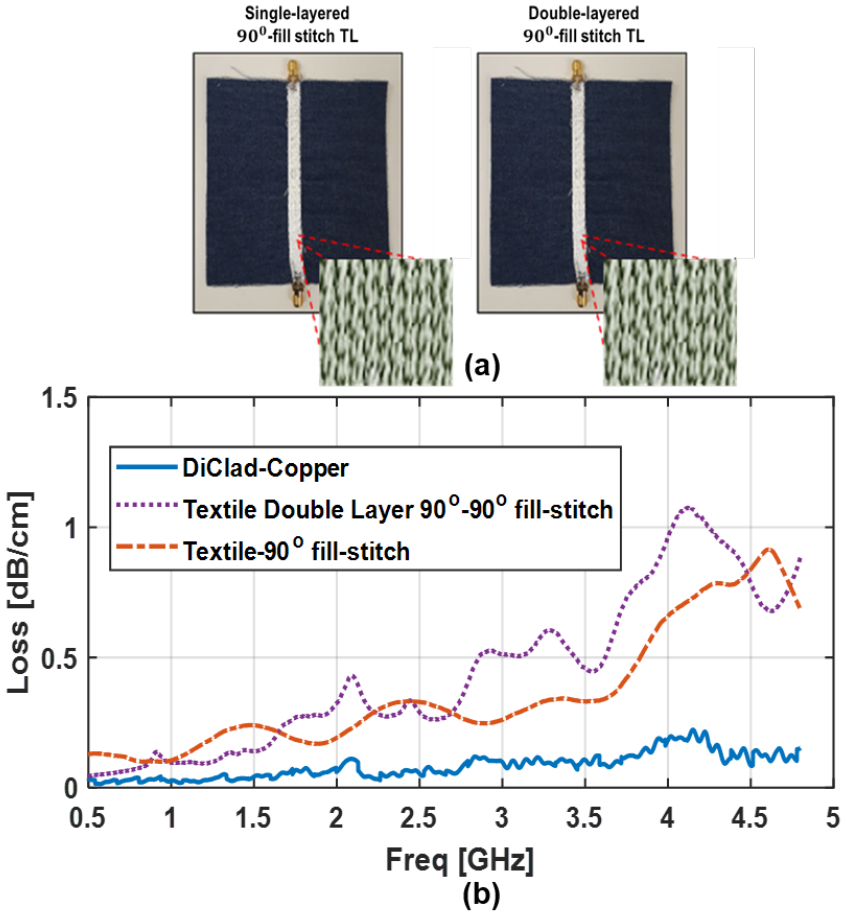


Figure 10: Loss-comparison of the double-layered textile transmission lines compared with that of single-layered textile transmission lines - minimizing the loss is essential to improve the power conversion efficiency of the rectifier, and demonstrates the need for short matching networks in lossy energy harvesters: (a) photographs of embroidered transmission lines; (b) their measured insertion loss as a function of the fabrication parameters. (©2018 IEEE [50])

performance was deduced using the equation 1.

$$Loss_{dB/cm} = \frac{10 \times log(1 - |S_{11}|^2 - |S_{21}|^2)}{L_{stripline}} \tag{1}$$

The measured loss performance of the three textile MTLs was compared with that of the DiClad880 (used as a reference) and reported in Figure 9(b). This figure suggests that by aligning the conductive threads in the direction of the RF current (see Figure 8), the loss performance is improved by 0.7 dB/cm at 3.5 GHz over the cases where the conductive threads are embroidered at a $90^0$ and a $45^0$ angles with the RF current path [50]. It is worth noting that the 45°-fill stitch embroidery pattern shows intermediate loss performance. Compared to its copper MTL (cladded onto the DiClad880 substrate), the best performance was approximately 0.25 dB/cm for the transmission line. The conductivity of the trace made via $90^0$-fill stitch of conductive threads is, therefore, the closest to that of a copper-based transmission line. An investigation on improvement of the conductivity of the $90^0$-fill stitch transmission was considered. For that, a double layer of conductive threads embroidered onto fabric was considered. The process consisted of embroidering another layer of conductive threads (using the 90°-fill stitch pattern) on top of a textile MTL using the same stitching pattern (see Figure 10(a)). The loss performance was evaluated using the equation 1, compared with that of the single-layered MTL and reported in Figure 10(b). As can be seen from Figure 10(b), using two layers of conductive threads to make a textile MTL could have improved its loss performance. Overall, the 90°-fill stitch was found to be the optimal stitching pattern to embroider excellent textile transmission lines. In other words, aligning the conductive threads with the direction of the RF current will enable the path of least resistance. These results can be served as design and manufacturing guidelines

for the development of high-performance textile antennas and RF circuits for wearable applications [47, 48].

### 2.1.2 Effects of Mechanical Deformations on the RF Performance of Textile MTLs

The wearable devices will be worn by human beings subject to mechanical deformations like bending, twisting, and folding. In addition, one of the critical requirements is the resilience to mechanical deformations to ensure an intact RF performance. As the textile TTLs will be used in the implementation of textile antennas, circuits, and RF modules, a study of the effects of mechanical deformations (bending and twisting) on the performance of the TTLs was carried out. In addition to that, the choice of fabric substrates was investigated for its influence on the loss performance of the TTLs. As a result, the loss performance of the textile MTLs becomes a function of four unknowns. In this study, two different

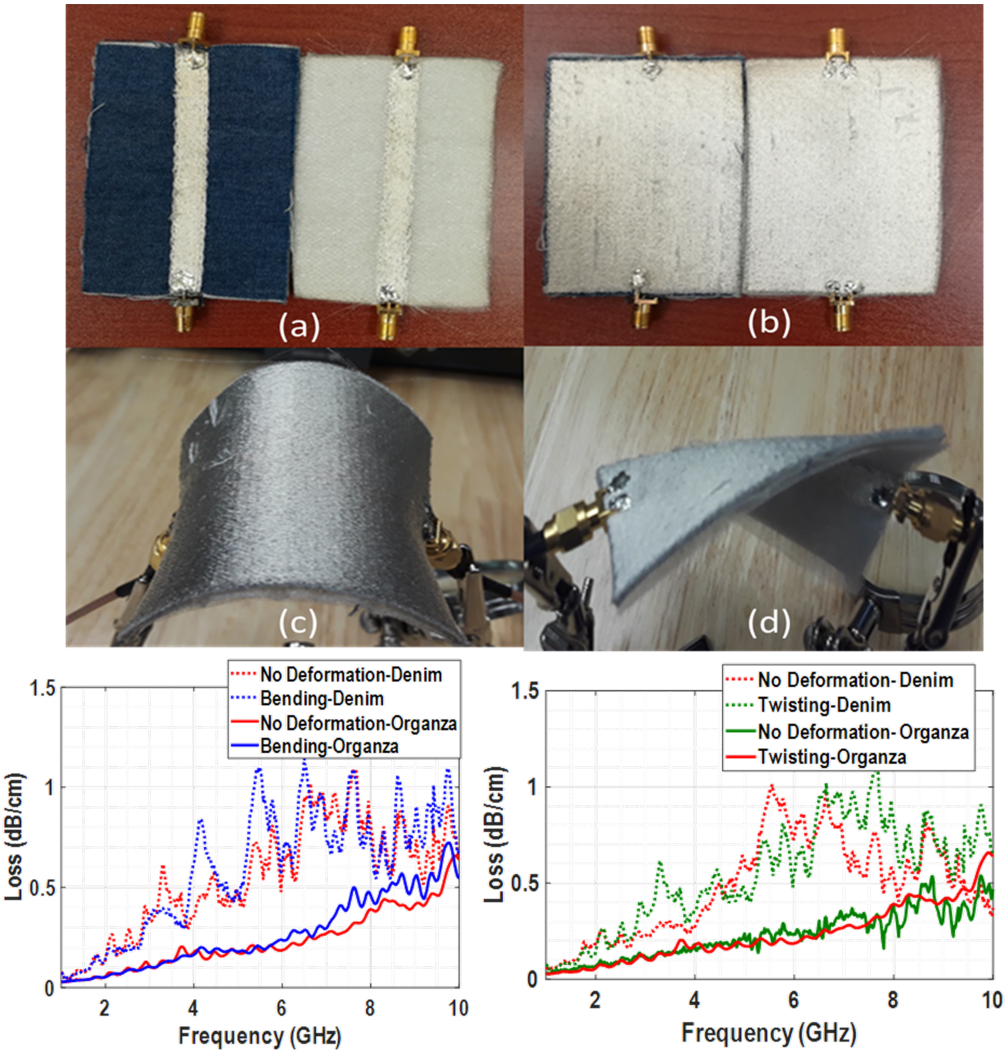


Figure 11: Effects of mechanical deformation on the performance of TTLs made of Elektrisola-7 embroidered onto denim and organza fabrics: (a) transmission line prototypes (for feeding the energy harvester) on textiles for wearable applications, (b) backside of the prototypes, (c) bending process of the samples, (d) twisting process of the samples, Bottom (left): loss performance due to bending, and Bottom (right): loss performance due to twisting. (©2019 IEEE [46])

substrates, denim and organza were considered, 90°-fill stitch (optimal embroidery pattern), and the TTLs underwent bending and twisting (mechanical deformations). The loss performance was evaluated from scattering parameters using the equation 1, and the measured results were reported in Figure 11. Two important embroidery parameters, namely, stitching density optimized to be 14 threads/mm and thread tension is chosen to be 4 (from a scale of 0 to 9). The design and fabrication processes were the same as previously discussed. Two textile transmission lines were prototyped where one was made of *Elektrisola-7* embroidered onto organza substrate ($\epsilon_r = 2.75$ and $\tan\delta = 0.0008$), and the other one,

made of *Elektrisola-7* embroidered onto denim ($\epsilon_r = 1.67$ and $\tan\delta = 0.07$). On the one hand, the results from Figure 11 (Bottom left and right) suggest that bending and twisting did not have an appreciable effect on the loss performance of the textile transmission lines [46]. On the other hand, it can be seen that the TTLs made of organza outperformed those made of denim. As a result, organza-based TTLs exhibited a loss of up to 0.6 dB/cm for frequencies of up to 10 GHz, while those made of denim suffered from a loss of 1.08 dB/cm for the same frequency range. When the TTLs were subject to mechanical deformations, no noticeable difference was found between bending and twisting. This suggests that embroidering 14 threads/mm, aligned in the direction of the RF current while maintaining the tension of the embroidery machine at 4, provides the best RF performance for textile transmission lines operating at frequencies of up to 10 GHz. In sum, the best design guideline for developing textile antennas and RF electronics/circuits is the embroidery of 14 Elektrisola-7 threads per millimeter of TTL length in the direction of the RF current onto organza fabric substrates while keeping the embroidery machine at a tension of 4.

Organza outperforms denim because organza can be seen as a cluster of grids where loss-induced agents like dust and moisture pass through without the possibility of sneaking within the voids to accumulate loss within the structures. However, denim is a cluster of cotton compartments that trap dust or moisture to accumulate loss within the structure. In order words, organza is the best candidate for the design guideline of textile RF modules due to its microstructure. As a result, by changing the substrate material from denim to organza, the loss performance of the TTLs can be improved by 0.5 dB/cm. So far, the best overall design guideline for the development of wearable devices is the use of *Elektrisola-7* threads embroidered longitudinally onto organza fabric while keeping the tension of the embroidery machine at 4.

Even though excellent RF performance was obtained for the design guideline mentioned above, the resulting prototypes' flexibility will be limited because the interconnections between the SMAs and the conductive traces were made of hard solder phases. Using a conductive material that is highly conductive and flexible is the ideal solution. In [49], Vital et al. presented the use of a special conductive epoxy (CM-127-48) from CreativeMaterials that achieved 50% of improvement in loss performance over its solder counterpart.

One of the essential applications for wearable is the internet of medical things or the internet of health things. Developing medical electronics for health purposes will require the ability of the device to be constantly in charge and consistently monitor the health status of the bearer. In addition, the bearer should be shielded from any potential radiation. The conductive materials listed above are suitable to shield against EM radiations.

## 2.2 Safety Consideration and Practical Deployment

The wearable devices aim to make the bearer independent when being worn for the intended application. Being independent underlines the use of these devices to perform tasks that would otherwise be performed by the bearer themselves. For that, the devices have to be self-powered and enable communication with outside [remote] receiver. In the case of medical devices, diagnosis, monitoring and treatment of illnesses, diseases, and disorders can be done in real-time. Powering these devices consists of developing textile-based wireless power transfer, harvesting, and sensing structures. This can be done by using the conductive materials listed above integrated with fabric-based and biocompatible flexible substrates. The wearable devices will receive and transmit RF signals for simultaneous wireless power and information transmission. Therefore, the bearer (human being) will be exposed to radiations and if not properly controlled, the latter can cause severe tissue damages. A quantitative representation of the human exposure to EM waves is the specific absorption rate (SAR) expressed through the following equation:

$$SAR = \sigma \frac{|E|^2}{\rho} \tag{2}$$

Where $\sigma$ is the conductivity of the tissue (S/m), $\rho$, is the mass density of the tissue (kg/$m^3$), and E is the RMS electric field strength (V/m). The international Commission on non-ionizing radiation protection (ICNIRP), the Institute of Electrical and Electronics Engineering (IEEE) and the Federal communications Commission (FCC) define the regulations pertaining to the development of wearable devices. The safety factor in the development of such devices is evaluated through the

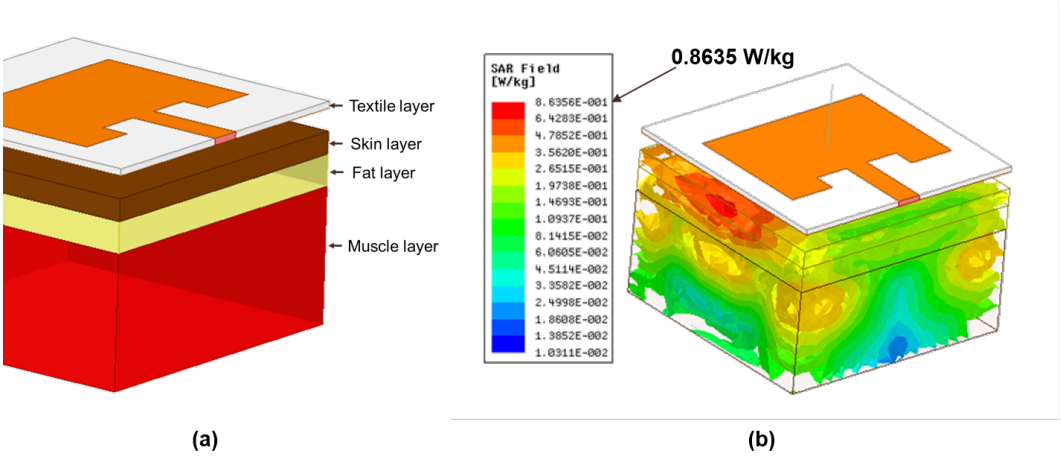


Figure 12: SAR level estimated in textile-based patch antenna for wearable applications at 2.45 GHz: (a) design model and human tissue represented by different layers and (b) the SAR value obtain from full wave simulation. (©2020 IEEE [47])

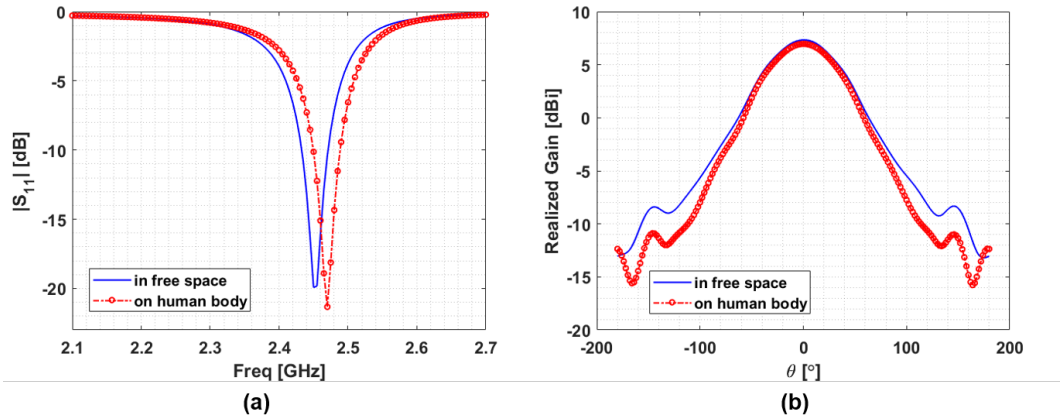


Figure 13: Results from full-wave simulation of textile patch antenna operated at 2.45 GHz in free space and on human body: (a) reflection coefficient and (b) realized gain (©2020 IEEE [47])

thermal distribution in human tissue (SAR) that can be calculated using equation (2) [12, 34]. This regulation is related to the transmitting power (1 W max) and the gain of the transmitting antenna (6 dB), which are combined into a 36-dBm EIRP. In addition, the IEEE requires a maximum SAR of 1.6 W/kg for exposure using 1 g and 10 g of tissue. The ICNIRP suggests an additional requirement of an incident power density of at most 10 W/$m^2$ for operating frequencies ranging from 30 MHz to 400 MHz, $f_M/40$ where $f_M$ in MHz for frequencies ranging from 400 MHz to 2 GHz, and 50 W/$m^2$ for frequencies ranging from 2 GHz to 300 GHz. To be in compliance with the SAR requlation, several design guidelines have been employed. One way is the use of a ground plane that separates the radiative surface of the device and the human tissue. The best examples of antennas (radiative elements) used for this technique is the patch antenna. This ground-plane-backed antenna will not only shield the human tissue from radiation, but also ensure no degradation in its gain and efficiency (see Figs. 12 & 13). The works published in [31, 47] show patch wearable patch antennas and arrays operating at 2.45 GHz and 5.8 GHz, and in [48] where an textile-based anchor-shaped antenna (see Figure 14) used in near-field wireless power transfer at 360 MHz exhibiting SAR levels within the FCC/IEEE/ICNIRP limit. Some antenna topologies do not inherently have ground planes and therefore, cannot exhibit a SAR level within the FCC limit. The review article by Guido and Kiourti, 2020 [16] reports a variety of antenna topologies that adopt some techniques to reduce their SAR levels for FCC compliance. Some of these methods rely on altering a ground plane placed underneath the antennas. Such method of modifying the ground plane is known as electromagnetic bandgap (EBG) or periodic conductive structures used to filter EM waves within certain frequency bands. Among the electromagnetic bandgap structures, some of them are used to reflect the EM waves away [13], dissipating electric field hot spots, or serves as a notch filter (to reject EM at some frequency band). Others inhibit the propagation of surface waves and phase-reversal reflections [16]. Besides reducing

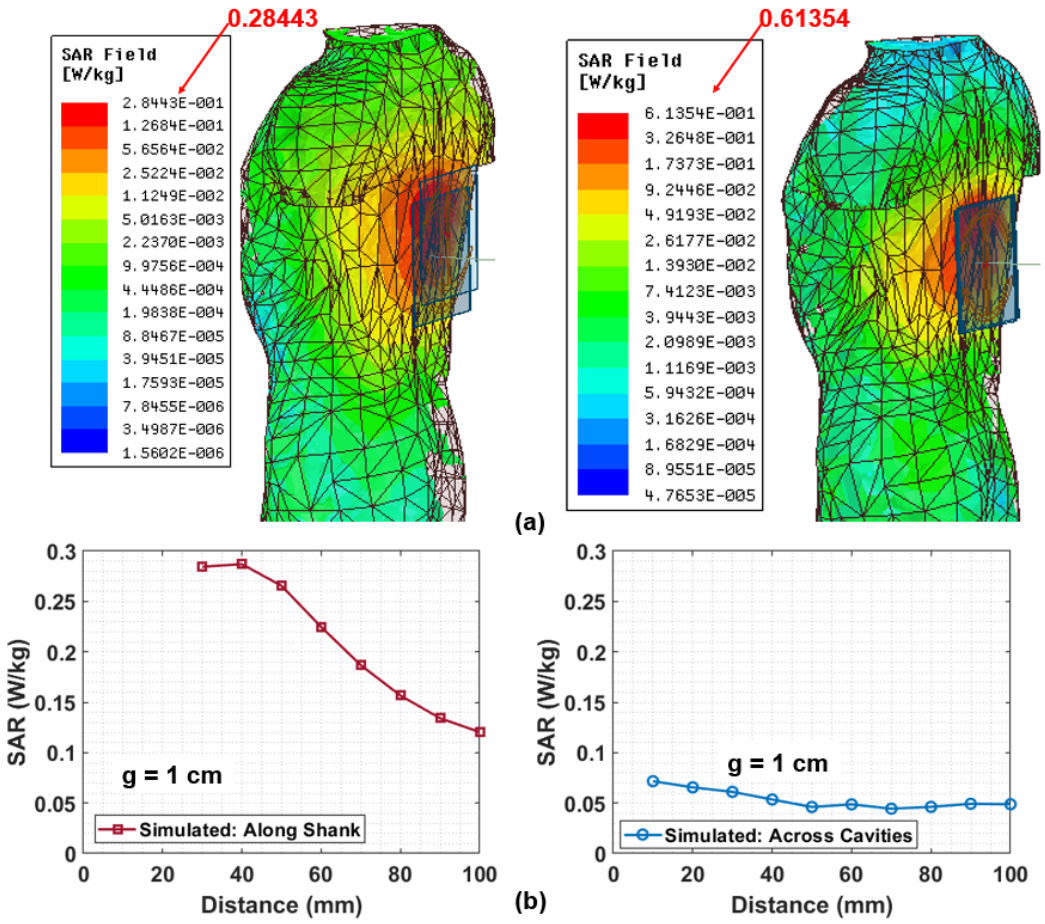


Figure 14: SAR values obtain from full-wave simulation of textile anchor antenna used for near-field wireless power transfer at 360 MHz for different misalignment scenarios: (a) SAR values obtained from a human torso and (b) different SAR values obtained in different locations on the human torso corresponding to the misalignment the antennas during the power transfer process. (©2021 IEEE [48])

the SAR elevels, the EBG also helps in improving power transmission (by 51%) in sensor-to-sensor communication [1], eliminate mismatch and frequency shifting caused by human body [5], reduce backlobe [45] and surface wave coupling [64]. Other structures can serve as isolators like artificial magnetic conductor (AMC) ground planes [3], and can also act like the main radiator in the case of the anisotropic metasurface [20]. These techniques have been demonstrated to reduce the SAR level by more than 99%. The reduction rate is calculated based on the following equation:

$$SAR_{reduction\ rate} = \left| \frac{SAR_{Initial} - SAR_{Final}}{SAR_{Initial}} \right| \times 100\% \tag{3}$$

where $SAR_{Initial}$ refers to the SAR evaluation when the antenna is measured alone and $SAR_{Final}$ when the techniques like EBG, AMC, metasuface, and HIS (high impedance surface) are integrated with the antenna. Table 1 reports different SAR reduction values resulted from the adoption of the techniques mentioned above. The incident power used for the SAR reduction methods reported in Table 1 was between 100 mW and 1 W and the SAR values were reduced from a value of 34.3 W/kg to as low as 0.0368 W/kg.

## 3 Emerging Systems and Applications

With the IoT and healthcare being at the forefront of WPT and RF energy harvesting applications, there are many research advances which can be combined to realize integrated sustainable sensing and communication systems with a low environmental impact. A few examples are highlighted in this section. **1. Epidermal electronics and sensors:** Given

Table 1: A comparison table of various techniques of SAR reduction compiled from the work published in [16] [AMC: artificial magnetic conductor, EBG: electromagnetic bandgap, and HIS: high impedance surface]

| References | Antenna Topology | Initial SAR Value / 1 g or 10 g ? | Method of SAR Reduction | SAR Reduction Rate | Frequency |
|---|---|---|---|---|---|
| Gao et al., 2018 [13] | PIFA | 7.23 W/kg [1 g] | 3 × 4 ring-shaped EBG | 98.74 % | 2.45 GHz |
| Zhu and Langley, 2009 [64] | Coplanar Antenna | 11.47 W/kg [1 g] | 3 × 3 EBG | 95.82 % | 1.8 GHz |
| Chen et Ku, 2016 [9] | Inverted L Antenna | 13.5 W/kg [1 g] | 2 × 2 Cross-shaped HIS | 97.85% | 2.4 GHz |
| Saeed et al., 2017 [40] | Reconfigurable Slot antenna | 2 W/kg [1 g] | Dual-band Polarization-dependent AMC | 85.5% | 2.45/ 3.3 GHz |
| Augustine et al., 2010 [6] | Integrated Inverted-F | 13.12 W/kg [1 g] | Polymeric Ferrite sheet | 89.02% | 2.4 GHz |
| Agarwal et al., 2016 [3] | Yagi-Uda | 34.3 W/kg [1 g] | Double-layered AMC | 94.72% | 2.45 GHz |
| Ashyap et al., 2017 [5] | Inverse E-shaped Monopole | 6.19 W/kg [1 g] | 2 × 2 EBG | 99.41% | 2.4 GHz |
| Abirami and Sundarsingh, 2017 [1] | Yagi-Uda | 8.73 W/kg [10 g] | 3 × 3 EBG | 99.08% | 2.4 GHz |
| Velan et al., 2015 [45] | Fractal Monopole | 6.62 W/kg [10 g] | 3 × 3 square slotted EBG | 99.76% | 2.45 GHz |
| Jiang et al., 2014 [20] | Monopole | 6.62 W/kg [1 g] | 2 × 2 Anisotropic Metasurface | 95.3% | 2.4 GHz |

the great promise of using flexible, printable, and sustainably-fabricated wearable-friendly circuits in power-autonomous healthcare, WPT continues to be applied in different epidermal applications. Both near-field [17] and surface-wave [43] body-scale metamaterials have been reported as a means of powering wearable devices sustainably. Such hybrid quasi-wireless approaches have shown promise as a low-loss alternative to radiative means while retaining some of the spatial freedom of far-field radiative WPT.

Epidermal and all-flexible systems typically rely on the hybrid integration of commercial discrete semiconductors with large-area components such as energy storage [62] and antennas [51]. Minimizing the dependence of such systems on high-environmental impact ICs can significantly contribute to lowering their footprint, where multiple low-temperature devices based on abundant elements can be printed for such transient RF-powered electronic systems.

**2. Computational RFID and Edge Computers:** Shortly after the wide-scale adoption of RFID as an inventory-tracking and wireless "barcode" technology, the concept of integrating computational functionality in RFID tags followed [61]. In this context, it is key to remember that a long-range far-field UHF RFID tag is effectively a rectenna with the rectifier and digital transponder integrated on the same small footprint IC. Computational RFID was demonstrated by Sample *et al.* [41] based on commercially-available MCUs and an RF power harvesting integrated on the same compact PCB. Leveraging the advances in low-power computing such as low-voltage micro-controllers [33].

**3. Autonomous Small Systems:** The concept of smart dust first appeared in the 1990s and relied on photovoltaics for power and optical communication for data transmission [21]. However, next-generation autonomous systems require more stable power supplies such as dedicated wireless transmission for applications like swarm robotics [18]. Wireless-powered miniaturized drones have recently been demonstrated [35], showing how RF WPT can generate the highest reported power-to-mass density, which can be applied in highly constrained small systems. The sustainable existence of such small autonomous electronic systems in future 6G networks will leverage the advances in WPT ranging from efficient RF power generation and transmission to device-level rectification and energy storage.

**4. Space Solar Power (SSP):** The concept of beaming microwave energy from kilometer-scale satellites emerged in the late 1960s and has been extensively researched by several space agencies around the world. This proposition is

highly attractive as the power generated in space will have zero environmental potential and can be directed to the desired location without the need for a local power grid. [39]. Despite being researched for over 50 years, there are still several unresolved practical challenges such as frequency allocations to the SSP satellites as well as the safety mechanisms deployed in such systems. However, it is anticipated that this area will seen an increase in research activities on the road to net-zero.

# 4 Summary and Conclusions

In the chapter, the key research advances and challenges in RF energy harvesting and wireless power technologies have been discussed. To ensure that 6G-enabled WPT contributes to net-zero, both the end-to-end efficiency and the environmental footprint, from cradle to grave, of WPT systems must be carefully considered. Across µW to MW applications, it is expected that WPT will have a crucial role in achieving net-zero. In addition to the device- and component-level challenges, this chapter highlighted some application domains, such as wearable and human-centric systems, where WPT can enable more user-friendly as well as sustainable electronic systems to be realized.

# References


[1] B. Sakthi Abirami and Esther Florence Sundarsingh. Ebg-backed flexible printed yagi–uda antenna for on-body communication. *IEEE Transactions on Antennas and Propagation*, 65(7):3762–3765, 2017.

[2] Salah-Eddine Adami, Plamen Proynov, Geoffrey S. Hilton, Guang Yang, Chunhong Zhang, Dibin Zhu, Yi Li, Steve P. Beeby, Ian J. Craddock, and Bernard H. Stark. A Flexible 2.45-GHz Power Harvesting Wristband With Net System Output From -24.3 dBm of RF Power. *IEEE Trans. Microw. Theory Techn.*, 66 no. 1:380–395, 2018.

[3] Kush Agarwal, Yong-Xin Guo, and Budiman Salam. Wearable amc backed near-endfire antenna for on-body communications on latex substrate. *IEEE Transactions on components, packaging and manufacturing technology*, 6(3):346–358, 2016.

[4] Abdullah S. Almansouri, Mahmoud H. Ouda, and Khaled N. Salama. A cmos rf-to-dc power converter with 86% efficiency and -19.2-dbm sensitivity. *IEEE Trans. Microw. Theory Techn.*, 66, 5:2409 – 2415, 2018.

[5] Adel YI Ashyap, Zuhairiah Zainal Abidin, Samsul Haimi Dahlan, Huda A Majid, Shaharil Mohd Shah, Muhammad Ramlee Kamarudin, and Akram Alomainy. Compact and low-profile textile ebg-based antenna for wearable medical applications. *IEEE Antennas and Wireless Propagation Letters*, 16:2550–2553, 2017.

[6] Robin Augustine, T Alves, T Sarrebourse, B Poussot, KT Mathew, Jean-Marc Laheurte, et al. Polymeric ferrite sheets for sar reduction of wearable antennas. *Electronics letters*, 46(3):197, 2010.

[7] Constantine A. Balanis. Antenna Theory: Analysis and Design. Third Edition. *Wiley Interscience*, pages 84 – 85, 2005.

[8] W.C. Brown. The history of power transmission by radio waves. *IEEE Transactions on Microwave Theory and Techniques*, 32(9):1230–1242, 1984.

[9] Yen-Sheng Chen and Ting-Yu Ku. A low-profile wearable antenna using a miniature high impedance surface for smartwatch applications. *IEEE Antennas and Wireless Propagation Letters*, 15:1144–1147, 2015.

[10] Bruno Clerckx, Alessandra Costanzo, Apostolos Georgiadis, and Nuno Borges Carvalho. Wireless Power Transmission: From Far Field to Near Field. *IEEE Microw. Mag.*, 19, 6:69 – 82, 2018.

[11] Yun Fang, Wei Hong, and Hao Gao. Analysis of mm-wave multi-stage rectifier and implementation. *IEEE Transactions on Microwave Theory and Techniques*, 70(10):4491–4501, 2022.

[12] Radiofrequency Electromagnetic Fields. Evaluating compliance with fcc guidelines for human exposure to radiofrequency electromagnetic fields. *OET bulletin*, 65(10), 1997.

[13] Guoping Gao, Bin Hu, Shaofei Wang, and Chen Yang. Wearable planar inverted-f antenna with stable characteristic and low specific absorption rate. *Microwave and Optical Technology Letters*, 60(4):876–882, 2018.

[14] Dimitra G. Georgiadou, James Semple, Abhay A. Sagade, Henrik Forstén, Pekka Rantakari, Yen-Hung Lin, Feras Alkhalil, Akmaral Seitkhan, Kalaivanan Loganathan, Hendrik Faber, and Thomas D. Anthopoulos. 100 GHz zinc oxide Schottky diodes processed from solution on a wafer scale. *Nature Electronics*, 3:718–725, 2020.

[15] Xiaoqiang Gu, Simon Hemour, and Ke Wu. Far-Field Wireless Power Harvesting: Nonlinear Modeling, Rectenna Design, and Emerging Applications. *Proceedings of the IEEE*, 110(1):56–73, 2022.

[16] Katrina Guido and Asimina Kiourti. Wireless wearables and implants: A dosimetry review. *Bioelectromagnetics*, 41(1):3–20, 2020.

[17] Amirhossein Hajiaghajani, Amir Hosein Afandizadeh Zargari, Manik Dautta, Abel Jimenez, Fadi Kurdahi, and Peter Tseng. Textile-integrated metamaterials for near-field multibody area networks. *Nat. Electron.*, 2021.

[18] Simon Hemour, Carlos H. P. Lorenz, and Ke Wu. Small-footprint wideband 94 GHz rectifier for swarm micro-robotics. In *2015 IEEE MTT-S International Microwave Symposium*, 2015.

[19] Suk-Won Hwang, Xian Huang, Jung-Hun Seo, Jun-Kyul Song, Stanley Kim, Sami Hage-Ali, Hyun-Joong Chung, Hu Tao, Fiorenzo G. Omenetto, Zhenqiang Ma, and John A. Rogers. Materials for bioresorbable radio frequency electronics. *Advanced Materials*, 25(26):3526–3531, 2013.

[20] Zhi Hao Jiang, Donovan E Brocker, Peter E Sieber, and Douglas H Werner. A compact, low-profile metasurface-enabled antenna for wearable medical body-area network devices. *IEEE Transactions on antennas and propagation*, 62(8):4021–4030, 2014.

[21] J. M. Kahn, R. H. Katz, and K. S. J. Pister. Next century challenges: mobile networking for "smart dust". In *Proceedings of the 5th annual ACM/IEEE international conference on Mobile computing and networking*, MobiCom '99, page 271–278, New York, NY, USA, Aug 1999. Association for Computing Machinery.

[22] Hooman Kazemi. 61.5% efficiency and 3.6 kw/m2 power handling rectenna circuit demonstration for radiative millimeter wave wireless power transmission. *IEEE Transactions on Microwave Theory and Techniques*, 70(1):650–658, 2022.

[23] Talha Ahmed Khan, Ahmed Alkhateeb, and Robert W. Heath. Millimeter Wave Energy Harvesting. *IEEE Trans. Wireless Communications*, 15, 9:6048 – 6062, 2016.

[24] P. Koert and J.T. Cha. Millimeter wave technology for space power beaming. *IEEE Trans. Mirow Theory Techn.*, 40 no. 6:1251 – 1258, 1992.

[25] Koji Kotani, Atsushi Sasaki, and Takashi Ito. High-efficiency differential-drive cmos rectifier for uhf rfids. *IEEE Journal of Solid-State Circuits*, 44(11):3011–3018, 2009.

[26] Shabnam Ladan, Ajay Babu Guntupalli, and Ke Wu. A High-Efficiency 24 GHz Rectenna Development Towards Millimeter-Wave Energy Harvesting and Wireless Power Transmission. *IEEE Trans. Circuits And Systems*, 61, 12:3358 – 3366, 2014.

[27] Agnieszka Lekawa-Raus, Jeff Patmore, Lukasz Kurzepa, John Bulmer, and Krzysztof Koziol. Electrical properties of carbon nanotube based fibers and their future use in electrical wiring. *Advanced Functional Materials*, 24(24):3661–3682, 2014.

[28] Wei Lin, Richard W. Ziolkowski, and Jianquan Huang. Electrically small, low-profile, highly efficient, huygens dipole rectennas for wirelessly powering internet-of-things devices. *IEEE Transactions on Antennas and Propagation*, 67(6):3670–3679, 2019.

[29] Kalaivanan Loganathan, Hendrik Faber, Emre Yengel, Akmaral Seitkhan, Azamat Bakytbekov, Emre Yarali, Begimai Adilbekova, Afnan AlBatati, Yuanbao Lin, Zainab Felemban, Shuai Yang, Weiwei Li, Dimitra G. Georgiadou, Atif Shamim, Elefterios Lidorikis, and Thomas D. Anthopoulos. Rapid and up-scalable manufacturing of gigahertz nanogap diodes. *Nature Communications*, 13:3260, 2022.

[30] Ping Lu, Chaoyun Song, and Ka Ma Huang. A Two-Port Multi-Polarization Rectenna with Orthogonal Hybrid Coupler for Simultaneous Wireless Information and Power Transfer (SWIPT). *IEEE Trans. Antennas Propag.*, 68 no. 10:6893 – 6905, 2020.

[31] Chun-Xu Mao, Dieff Vital, Douglas H Werner, Yuhao Wu, and Shubhendu Bhardwaj. Dual-polarized embroidered textile armband antenna array with omnidirectional radiation for on-/off-body wearable applications. *IEEE Transactions on Antennas and Propagation*, 68(4):2575–2584, 2019.

[32] Gaetano Marrocco. The art of UHF RFID antenna design: impedance-matching and size-reduction techniques. *IEEE Antennas Propag. Magazine*, 50, 1:66 – 79, 2008.

[33] James Myers, Anand Savanth, Rohan Gaddh, David Howard, Pranay Prabhat, and David Flynn. A Subthreshold ARM Cortex-M0+ Subsystem in 65 nm CMOS for WSN Applications with 14 Power Domains, 10T SRAM, and Integrated Voltage Regulator. *IEEE Journal of Solid-State Circuits*, 51, 1:31 – 44, 2016.

[34] International Commission on Non-Ionizing Radiation Protection et al. Guidelines for limiting exposure to electromagnetic fields (100 khz to 300 ghz). *Health physics*, 118(5):483–524, 2020.

[35] Takashi Ozaki, Norikazu Ohta, Tomohiko Jimbo, and Kanae Hamaguchi. A wireless radiofrequency-powered insect-scale flapping-wing aerial vehicle. *Nature Electronics*, 4(11):845–852, Nov 2021.

[36] Valentina Palazzi, Jimmy Hester, Jo Bito, Federico Alimenti, Christos Kalialakis, Ana Collado, Paolo Mezzanotte, Apostolos Georgiadis, Luca Roselli, and Manos M. Tentzeris. A Novel Ultra-Lightweight Multiband Rectenna on Paper for RF Energy Harvesting in the Next Generation LTE Bands. *IEEE Trans. Microw. Theory Techn.*, 66 no. 1:366 –379, 2018.

[37] Tharindu D. Ponnimbaduge Perera, Dushantha Nalin K. Jayakody, Shree Krishna Sharma, Symeon Chatzinotas, and Jun Li. Simultaneous Wireless Information and Power Transfer (SWIPT): Recent Advances and Future Challenges. *IEEE Communication Surveys and Tutorials*, 20, 1:264 – 302, 2018.

[38] Manuel Pinuela, Paul D. Mitcheson, and Stepan Lucyszyn. Ambient RF Energy Harvesting in Urban and Semi-Urban Environments. *IEEE Trans. Microw. Theory Techn.*, 61 no. 7:2715 – 2726, 2013.

[39] Christopher T. Rodenbeck, Paul I. Jaffe, Bernd H. Strassner II, Paul E. Hausgen, James O. McSpadden, Hooman Kazemi, Naoki Shinohara, Brian B. Tierney, Christopher B. DePuma, and Amanda P. Self. Microwave and millimeter wave power beaming. *IEEE Journal of Microwaves*, 1(1):229–259, 2021.

[40] Saud M Saeed, Constantine A Balanis, Craig R Birtcher, Ahmet C Durgun, and Hussein N Shaman. Wearable flexible reconfigurable antenna integrated with artificial magnetic conductor. *IEEE Antennas and Wireless Propagation Letters*, 16:2396–2399, 2017.

[41] Alanson P. Sample, Daniel J. Yeager, Pauline S. Powledge, Alexander V. Mamishev, and Joshua R. Smith. Design of an rfid-based battery-free programmable sensing platform. *IEEE Transactions on Instrumentation and Measurement*, 57(11):2608–2615, 2008.

[42] Hucheng Sun, Yong xin Guo, Miao He, and Zheng Zhong. Design of a High-Efficiency 2.45-GHz Rectenna for Low-Input-Power Energy Harvesting. *IEEE Antennas Wireless Propag. Lett.*, 11:929–932, 2012.

[43] Xi Tian, Pui Mun Lee, Yu Jun Tan, Tina L. Y. Wu, Haicheng Yao, Mengying Zhang, Zhipeng Li, Kian Ann Ng, Benjamin C. K. Tee, and John S. Ho. Wireless body sensor networks based on metamaterial textiles. *Nature Electronics*, 2:243–251, 2019.

[44] Christopher R. Valenta and Gregory D. Durgin. Harvesting Wireless Power: Survey of Energy-Harvester Conversion Efficiency in Far-Field, Wireless Power Transfer Systems. *IEEE Microw. Mag.*, 15, 4:108–120, 2014.

[45] Sangeetha Velan, Esther Florence Sundarsingh, Malathi Kanagasabai, Aswathy K Sarma, Chinnambeti Raviteja, Ramprabhu Sivasamy, and Jayaram Kizhekke Pakkathillam. Dual-band ebg integrated monopole antenna deploying fractal geometry for wearable applications. *IEEE antennas and wireless propagation letters*, 14:249–252, 2014.

[46] Dieff Vital, Shubhendu Bhardwaj, and John L Volakis. Bending and twisting tests for rf performances of textile transmission lines. In *2019 IEEE International Symposium on Antennas and Propagation and USNC-URSI Radio Science Meeting*, pages 2173–2174. IEEE, 2019.

[47] Dieff Vital, Shubhendu Bhardwaj, and John L Volakis. Textile-based large area rf-power harvesting system for wearable applications. *IEEE Transactions on Antennas and Propagation*, 68(3):2323–2331, 2019.

[48] Dieff Vital, Pawan Gaire, Shubhendu Bhardwaj, and John L Volakis. An ergonomic wireless charging system for integration with daily life activities. *IEEE Transactions on Microwave Theory and Techniques*, 69(1):947–954, 2020.

[49] Dieff Vital, Md Monirojjaman Monshi, Shubhendu Bhardwaj, P Markondeya Raj, and John L Volakis. Flexible ink-based interconnects for textile-integrated rf components. In *2020 IEEE International Symposium on Antennas and Propagation and North American Radio Science Meeting*, pages 151–152. IEEE, 2020.

[50] Dieff Vital, Jingni Zhong, Shubhendu Bhardwaj, and John L Volakis. Loss-characterization and guidelines for embroidery of conductive textiles. In *2018 IEEE International Symposium on Antennas and Propagation & USNC/URSI National Radio Science Meeting*, pages 1301–1302. IEEE, 2018.

[51] M. Wagih, N. Hillier, S. Yong, A. S. Weddell, and S. Beeby. Rf-powered wearable energy harvesting and storage module based on e-textile coplanar waveguide rectenna and supercapacitor. *IEEE Open Journal of Antennas and Propagation*, 2:302 – 314, 2021.

[52] Mahmoud Wagih and Steve Beeby. Thin flexible rf energy harvesting rectenna surface with a large effective aperture for sub w/cm2 powering of wireless sensor nodes. *IEEE Transactions on Microwave Theory and Techniques*, 70(9):4328–4338, 2022.

[53] Mahmoud Wagih, Geoffrey S. Hilton, Alex S. Weddell, and Steve Beeby. 2.4 GHz Wearable Textile Antenna/Rectenna for Simultaneous Information and Power Transfer. In *2021 15th European Conference on Antennas and Propagation (EuCAP)*, pages 1–5, 2021.

[54] Mahmoud Wagih, Geoffrey S. Hilton, Alex S. Weddell, and Steve Beeby. Dual-Band Dual-Mode Textile Antenna/Rectenna for Simultaneous Wireless Information and Power Transfer (SWIPT). *IEEE Transactions on Antennas and Propagation*, 69(10):6322–6332, 2021.

[55] Mahmoud Wagih, Geoffrey S. Hilton, Alex S. Weddell, and Steve Beeby. Dual-Polarized Wearable Antenna/Rectenna for Full-Duplex and MIMO Simultaneous Wireless Information and Power Transfer (SWIPT). *IEEE Open Journal of Antennas and Propagation*, 2:844–857, 2021.

[56] Mahmoud Wagih, Geoffrey S. Hilton, Alex S. Weddell, and Steve Beeby. Higher-Order Mode Broadband Textile-Based Microstrip Antenna for Compact Wearable Millimeter-Wave Wireless Power Transfer. *IEEE Open Journal of Antennas and Propagation*, (Under Review).

[57] Mahmoud Wagih, Alex S. Weddell, and Steve Beeby. High-Efficiency Sub-1 GHz Flexible Compact Rectenna based on Parametric Antenna-Rectifier Co-Design. In *2020 IEEE/MTT-S International Microwave Symposium (IMS)*, 2020.

[58] Mahmoud Wagih, Alex S. Weddell, and Steve Beeby. Meshed High-Impedance Matching Network-Free Rectenna Optimized for Additive Manufacturing. *IEEE Open Journal of Antennas and Propagation*, 1:615 – 626, 2020.

[59] Mahmoud Wagih, Alex S. Weddell, and Steve Beeby. Millimeter-Wave Power Harvesting: A Review. *IEEE Open Journal of Antennas and Propagation*, 1:560 – 578, 2020.

[60] Mahmoud Wagih, Alex S. Weddell, and Steve Beeby. Rectennas for RF Energy Harvesting and Wireless Power Transfer: a Review of Antenna Design [Antenna Applications Corner]. *IEEE Antennas Propag. Mag.*, 62 no. 5:95 – 107, 2020.

[61] R. Want. Enabling ubiquitous sensing with rfid. *Computer*, 37(4):84–86, 2004.

[62] Lu Yin, Mengzhu Cao, Kyeong Nam Kim, Muyang Lin, Jong-Min Moon, Juliane R. Sempionatto, Jialu Yu, Ruixiao Liu, Connor Wicker, Alexander Trifonov, Fangyu Zhang, Hongjie Hu, Jose R. Moreto, Jaekyung Go, Sheng Xu, and Joseph Wang. A stretchable epidermal sweat sensing platform with an integrated printed battery and electrochromic display. *Nature Electronics*, 5(10):694–705, Oct 2022.

[63] Xu Zhang, Jesús Grajal, Jose Luis Vazquez-Roy, Ujwal Radhakrishna, Xiaoxue Wang, Winston Chern, Lin Zhou, Yuxuan Lin, Pin-Chun Shen, Xiang Ji, Xi Ling, Ahmad Zubair, Yuhao Zhang, Han Wang, Madan Dubey, Jing Kong, Mildred Dresselhaus, and Tomás Palacios. Two-dimensional MoS2-enabled flexible rectenna for Wi-Fi-band wireless energy harvesting. *Nature*, 566:368–372, 2019.

[64] Shaozhen Zhu and Richard Langley. Dual-band wearable textile antenna on an ebg substrate. *IEEE transactions on Antennas and Propagation*, 57(4):926–935, 2009.